TRANSPORT PROBLEMS 2024 Volume 19 Issue 4
PROBLEMY TRANSPORTU DOI: 10.20858/tp.2024.19.4.06

Keywords: machine learning; diesel engines; emissions prediction; artificial neural networks; fuel variability; environmental regulations; predictive modeling

Jonas MATIJOŠIUS*[1], Alfredas RIMKUS[2], Alytis GRUODIS[3]

PREDICTION OF THE MAIN ENVIRONMENTAL AND ENERGY CHARACTERISTICS OF DIESEL ENGINES USING AN ARTIFICIAL NEURAL NETWORK FOR PURE DIESEL FUEL, PURE HVO, AND A MIXTURE OF THESE FUELS IN THE RATIO 50/50 BY VOLUME

Summary. This research assesses the influence of different quantities of hydrotreated vegetable oil (HVO) in diesel fuel on the performance of the engine and the emissions it produces. The particular areas of interest are the level of smoke emitted and the brake thermal efficiency (BTE). A series of engine experiments were undertaken to quantify emissions and performance characteristics under various operating regimes using three distinct fuel blends: D100 (pure diesel), HVO50 (50% HVO mixture), and HVO100 (pure HVO). The results show a tendency to reduce soot emissions when the amount of HVO in the mixture reaches 50%, but in order to accurately determine the correlation between the amount of HVO and emissions, additional studies with various concentrations of HVO and diesel mixtures are necessary. Similarly, the results show a slight improvement in BTE stability with a 50% HVO blend, but more studies with different percentages of HVO-diesel blends are needed to reliably determine changes in BTE. This indicates a trend of change in engine performance with increasing HVO concentration in diesel fuel. In order to forecast emissions and performance indicators under different operating scenarios, we used artificial neural networks ANNs, which demonstrated excellent prediction accuracy, exhibiting robust linear correlations between the expected and real values for all fuel types. This research emphasizes the advantages of utilizing HVO in diesel engines for both environmental impact and performance. It also emphasizes the usefulness of ANNs in optimizing engine settings to improve efficiency and minimize emissions. The results endorse the further use of HVO as a viable substitute for conventional diesel, leading to less ecological consequences and enhanced engine efficiency.

1. INTRODUCTION

In transportation, the usage of hydrotreated vegetable oil (HVO) in diesel is very important for several reasons: due to regulatory compliance [1], for environmental benefits [2], for improved performance [3], and due to market demand [4]. Many countries (for example, in the EU) have governmental regulations for i) reducing greenhouse gas emissions and ii) promoting the use of ecologically friendly products [5]. As a renewable alternative to traditional diesel fuel, HVO emits lower levels of technical pollutants such as carbon monoxide (CO) and hydrocarbons (HC) [6]. For environmental sustainability, increasing the amount of HVO in diesel reduces emissions. Mixing HVO and fossil fuels allows compliance with these rules over a wide range of applications [7]. In the

[1] Vilnius College of Higher Education, Technical Faculty; Olandu 16, LT-01100 Vilnius, Lithuania; e-mail: j.matijosius@vtdko.lt; orcid.org/0000-0001-6006-9470
[2] Vilnius College of Higher Education, Technical Faculty; Olandu 16, LT-01100 Vilnius, Lithuania; e-mail: a.rimkus@vtdko.lt; orcid.org/0000-0001-8995-7180
[3] Mykolas Romeris University, Faculty of Public Governance and Business; Ateities 20, LT-08303 Vilnius, Lithuania; e-mail: alytis.gruodis@mruni.eu; orcid.org/0000-0001-8622-597X
* Corresponding author. E-mail: j,matijosius@tef.viko.lt

framework of improved performance of diesel engines, usage of HVO can significantly increase the power output and engine longevity [8]. Due to higher cetane numbers compared to traditional diesel, HVO-containing fuel burns more cleanly, resulting in smoother engine operation and better fuel economy [9, 10]. Consumer demand for organic products (including transport fuel) is growing [11, 12]. By offering mixtures of diesel with higher HVO content, transport companies can meet this demand and increase their market competitiveness.

Generally, adjusting the amount of HVO in diesel for transportation purposes can bring about a range of benefits, including improved performance, environmental protection, and regulatory compliance. The amount of HVO in diesel is not a solved problem. The usage of commercially available diesel containing 10%, 30%, 40%, and 50% HVO supplements (HVO10, HVO30, HVO40, HVO50) shows several benefits in the plane of ecology (decreased levels of pollutants). However, different energetical regimes of diesel engines may not be related to the linear dependence of outcome distributions. More strictly, the prognosis and prediction of pollutants of diesel engines working at large intervals of different regimes is a very complicated task that could be solved in an approximating way using artificial neural network (ANN) algorithms [13].

This work is devoted to estimating the quality of ANN prognosis for several types of pollutants (smoke, CO_2, NO_x) in diesel outcomes when diesel engine works in a wide range of regimes using different commercial fuels: D100 (pure diesel), HVO50 (containing 50% HVO supplement), and HVO100 (pure HVO).

a) To establish a relationship for chemical parameters (smoke, CO_2, NO_x) related to diesel working regime and fuel type (D100, HVO50, HVO100).
b) To establish a relationship for an energetic parameter (*BTE*) related to diesel working regime and fuel type (D100, HVO50, HVO100).
c) To estimate the parameters of ANN architecture and training regime for such type tasks of prognosis,
d) To estimate the prognosis precision for HVO-containing fuels.

Authors of publications in journals do not get honorarium and also agree with the publication of articles in the printed version of the journal and also on the internet version.

Recent advancements in predictive modeling for engine emissions have been significant. A study by [13] explored the relationship between engine power, vibrational and sound pressure levels, and exhaust emissions. It was found that engine power and the type of fuel significantly influence these variables, enhancing predictive models' capabilities for exhaust emissions. The root mean square (RMS) related function T11 was identified as a potent predictor within these models. Adding vibration data to these models not only enriched the dataset but also improved the accuracy of predicting emissions from biodiesel fuels.

In another study, the effectiveness of different predictive models was assessed on a single-cylinder four-stroke engine, with findings highlighting the model's accuracy (MAPE < 1%) across most engine emission parameters such as max_press, CA05, and CO, among others. However, certain emissions like NO_X remained challenging to predict, underscoring the need for developing new predictive techniques [14].

The role of machine learning, specifically ANNs, in predicting engine emissions has been increasingly recognized [15–17]. A particular study developed a 3-7-7-6 ANN model, integrating key combustion parameters to predict engine efficiency and emissions. This model demonstrated high accuracy with an R^2 close to unity and a low RMSE, indicating its potential to aid engine design and development [18]. Despite its efficacy, the need for updating neural network algorithms as engine parameters evolve remains a critical consideration.

Buscema [19] overviewed a feed-forward back propagation (BP) ANN. Buscema claimed that BP consisting of a single hidden layer is sufficient for mapping any function $y=f(x)$. Practically, deviations from a target value are too large, and it is sometimes necessary to expand the architecture of ANN and use an ANN consisting of double hidden layers. This happens when the functions to simulate are highly complex. Sekhar et al. [20] observed the working of BP by approximating the non-linear association between the data and the yield by changing the weight regards inside. Murat [21] used a learning/training algorithm of BP ANN. Zhang et al. [22] described the feed-forward neural networks with random

weights (FNNRWs). The main behavior is related to clusterization: FNN divides large-scale data into subsets of the same size, and each subset derives the corresponding sub-model. The presented approach demonstrates the successful acceptance of processing huge datasets.

The environmental implications of engine emissions are profound, contributing to natural disasters and climatic anomalies such as El Niño and forest fires. A broader perspective provided by [23] discusses the role of sustainable development goals set by the United Nations, emphasizing the importance of improving engine performance and reducing emissions through advanced machine learning techniques. These include not only ANNs but also other methods such as the relevance vector method, support vector machine, and genetic algorithms, which could further refine predictive accuracy and environmental sustainability.

2. METHODS AND MATERIALS

The experimental engine tests were carried out using the engine load bench and additional equipment as shown in Fig. 1. The engine used is a 1.9 TDI (VW) compression ignition four-stroke four-cylinder engine with air turbocharger and an air intercooler for which the EGR flow is cooled. The main technical characteristics of the engine are as follows: compression ratio 19.5, maximum power 66 kW (4000 rpm), maximum torque 180 Nm (2000–2500 rpm). The engine complies with the Euro 3 emission standard. The exhaust gas composition was measured before the oxidation catalyst.

Technical characteristics of the equipment used for the engine performance measurement: engine load bench (KI-5543) torque measurement accuracy ±1.2 Nm, fuel consumption scale (SK-5000) measurement accuracy ±1.0 g, air mass meter (BOSCH HFM 5) accuracy ±2%, exhaust gas analyzer (AVL DiCom 4000) measurement accuracy ±0.1% for CO_2, ±0.01% for CO, ±1 ppm for CH, ±1 ppm for NO_x and ±0.01% for smoke (opacity).

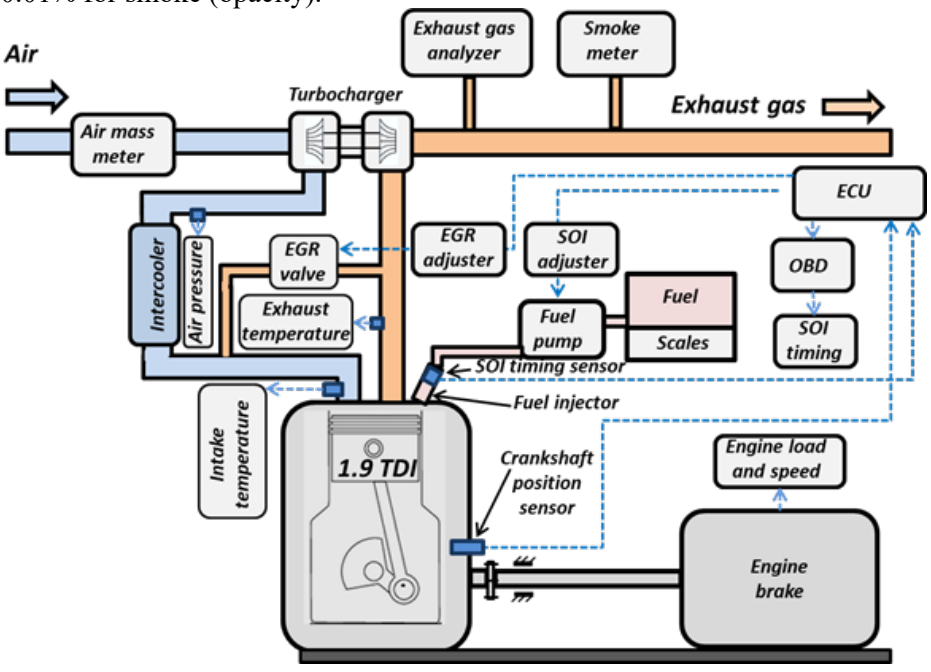

Fig. 1. Layout of engine performance test equipment

In order to investigate the wide range of engine performance, the tests are carried out with the engine running in different regimes where the start of injection (*SOI*) and exhaust gas recirculation (EGR) were adjusted by the electronic control unit (ECU), with the additional adjustments of *SOI* and EGR. *SOI* was measured with an accuracy of ±1.0 crank angle degree (CAD) by connecting Vag-Com diagnostic equipment to the onboard diagnostic port. The EGR ratio is defined as the mass fraction of exhaust gas

on the total inlet air + exhaust gas input. The EGR ratio is based on the mass measurement of the intake air. In this case, the mass of the EGR is determined by calculating the difference between the mass of the intake air when the EGR is on and when the EGR is off.

The experimental investigation of the engine was carried out in a rather narrow speed range, as it focused on the main operating modes of the engine in city driving. During the test, the engine speed was n = 2000 pm and n = 2500 rpm; torque was M_B = 30, 60, 90, and 120 Nm; *SOI* was 0–16 CAD before top dead center (bTDC); and EGR was 0–0.4. The conditions of the different regimes of testing are described in Fig. 2. The research is divided into seven working regimes (I–VII). RolNo represents an experimental event (numerated 0…173), which is related to the corresponding working regime characterized using technical parameters such as load and speed.

In Regimes I (events 0–21) and II (events 22–43), the engine load is changed (30, 60, 90, and 120 Nm) at speeds of 2000 rpm and 2500 rpm, when EGR and SOI are controlled by the engine ECU. In Regime III (events 44–67), the engine load is 60 Nm, the engine speed is 2000 rpm, the SOI is fixed, and the EGR is set to its default value (0.05, 0.10, 0.15, or 0.20). In Regime IV (events 68–91), the engine load is 60 Nm, the engine speed is 2000 rpm, the EGR is fixed at 0.15, and the SOI is set to the default values (0, 2, 4, 6, 8, 10, 12, 14, and 16 CAD bTDC). In Regime V (events 92–121), the engine load is changed (30, 60, 90, and 120 Nm), the engine speed is 2000 rpm, the EGR is controlled by the engine ECU (~0.4, ~0.3, ~0.25, and ~0.15), and the SOI is also controlled by the ECU (~2, ~3, ~4, and ~5 CAD bTDC). In Regime VI (events 122–137) the engine load is changed (30, 60, 90, and 120 Nm), the engine speed is 2500 rpm, the EGR is controlled by the engine ECU, and the SOI is also controlled by the ECU. In Regime VII (events 138–173), the engine load is 60 Nm, the engine speed is 2000 rpm, the EGR is fixed at 0.20, and the SOI is set to the default values (0, 2, 4, 6, 8, 10, 12, 14, and 16 CAD bTDC).

Tests were conducted using pure diesel (D100), pure biodiesel–hydrotreated vegetable oil (HVO100), and a mixture of diesel and HVO (50% by volume each), referred to as HVO50. The laboratory investigation focused on the physical and chemical properties of the fuel, with the findings detailed in Table 1.

The specific carbon dioxide emissions (SCO_2) have been calculated by taking into account the carbon dioxide concentration in the exhaust gas, the mass of the exhaust gas, and the engine power. The specific emissions of nitrogen oxides (SNO_x) were calculated similarly. Together with the smoke characteristics, these parameters best represent the combustion chemistry and environmental parameters of the engine when operating on different fuel blends. Braking thermal efficiency (*BTE*) results are presented to evaluate the energy efficiency.

3. SIMULATION SETUP

3.1. ANN architecture

ANN architecture and dynamic training mode determine the final performance of ANN and following quality of validation/prediction [24]. We implemented an ANN consisting of an input layer, a single hidden layer, and an output layer. Fig. 3 represents the ANN schema in the framework of *VALLUM01* [25].

A bias was included in the hidden layer to facilitate flexibility. The software package VALLUM01, which includes a graphical and user-friendly interface for input, output, and control, was built using the JAVA Eclipse framework. A normalization plugin was used to transform any actual value (pink) from the specified interval into the (0;1) range. The denormalization plugin works in reverse. The information flow progresses from the lower levels to the upper levels.

For the ANN, two typical classes from [26] were used: *Matrix* and *NeuralNetwork*. An *S*-shaped function (a sigmoidal function) was used:

$$\sigma(x) = 1/(1+e^{(-x)}) \tag{1}$$

Four organizational stages—a) selecting the number of input layers, b) establishing the number of hidden layers (single or double), c) adjusting the number of perceptrons in the single hidden layer (in this case), and d) requesting the number of output layers—are described in previous works [27, 28] and are used in this study without any changes.

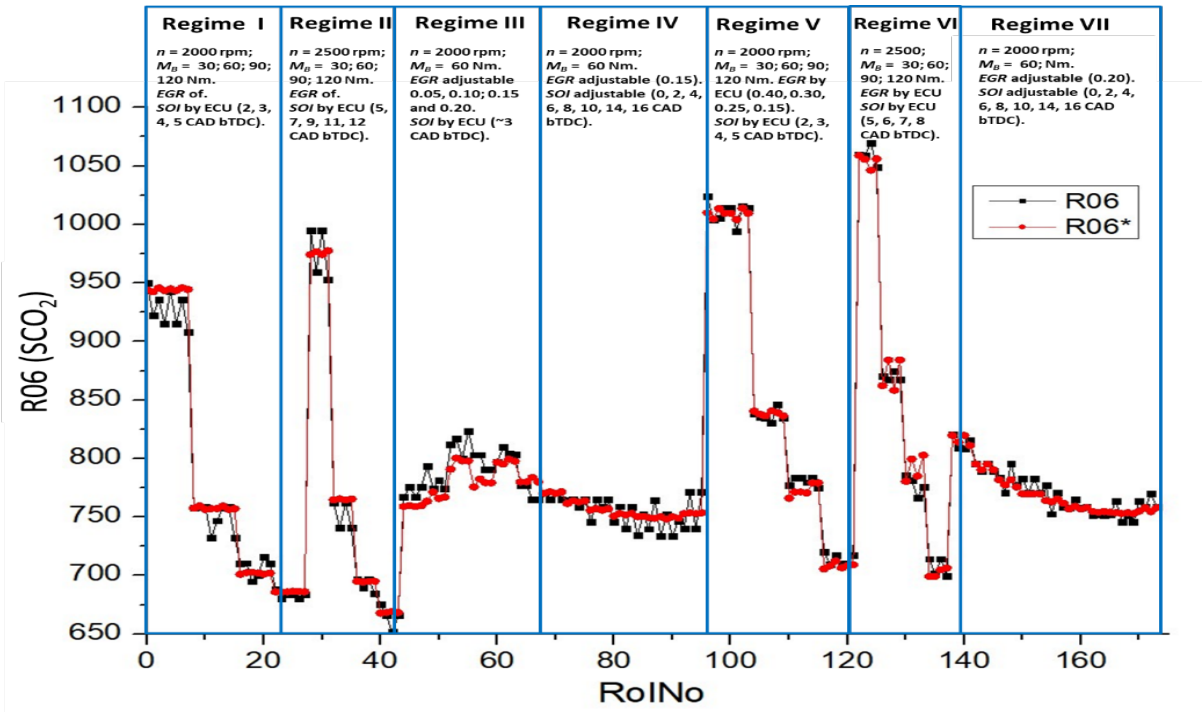

Fig. 2. Distribution of the output parameter (SCO_2) on experimental RolNo. Engine test regimes cover seven stages (I–VII). RolNo represents the experimental event characterized using technical parameters such as load and speed

Table 1

Fuel properties

Properties	D100	HVO50	HVO100
Kinematic viscosity at 40 °C, cSt	3.948	3.000	2.959
Dynamic viscosity, mPa · s	3.271	2.365	2.2617
Density at 15 °C, g/mL	0.830	0.806	0.780
Cetane number	50.9	59.9	74.5
C/H ratio	6.80	6.22	5.60
Air to fuel ratio (stoichiometric), kg air/1 kg fuel	14.50	14.79	15.10
Lower heating value (*LHV*), MJ/kg	42.82	43.21	43.63

3.2. Data collection

We established two input data clusters (refer to Table 2) and three output data clusters (refer to Table 3) according to analogous or relevant features for data collection. This framework helps reduce random fluctuations in the TNE. The artificial neural network consists of an input layer containing 12 units (yellow), a solitary hidden layer with M perceptrons (blue), and an output layer including 10 units (green) - refer to Fig. 3.

The first input cluster consists of parameters describing the technical conditions (P10, P03, P02, P11, P01), and the second input cluster consists of parameters describing burning chemistry parameters (P09, P04, P05, P12, P06, P08, P07) (see Table 3). The first output cluster consists of w SNO_x (R04). The

second output cluster consists of smoke (R00), and brake thermal efficiency (*BTE*) (R02). The third output cluster consists of SCO_2 (R06).

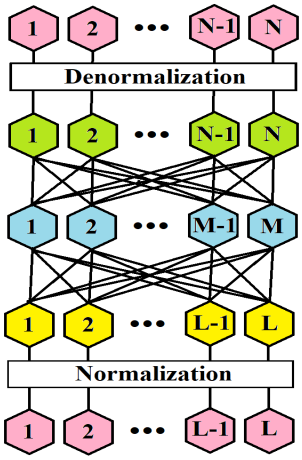

Fig. 3. Schematic diagram of an artificial neural network (ANN) architecture with normalization and denormalization layers. The ANN consists of an input layer with 12 units (yellow), a single hidden layer with 200 perceptrons (blue), and an output layer with 10 units (green). Normalization and denormalization plugins were applied for data conversion and reconversion. The data flow moves from the bottom to the top

Table 2

Experimental parameters of diesel engine used for an ANN as the input parameters

Cluster	Index	Abbr.	Parameter	Units	Interval	
					X_{MIN}	X_{MAX}
1	0	P10	The excess air ratio ($\boldsymbol{\lambda}$)	-	1.0	10.0
1	1	P03	Brake mean effective pressure (*BMEP*)	MPa	0.0	1.2
1	2	P02	*EGR* ratio	-	0.0	0.5
1	3	P11	Start of injection (*SOI*)	CA bTDC	−3.0	18.0
2	4	P09	Cetane number	-	5.0	85.0
1	5	P01	Engine speed (*n*)	rpm	800.0	4000.0
2	6	P04	Volume fraction of HVO100	%	0.0	100.0
2	7	P05	Volume fraction of D100	%	0.0	100.0
2	8	P12	C/H ratio	-	5.0	7.0
2	9	P06	Stoichiometric air-to-fuel ratio ($\boldsymbol{l_0}$)	1 kg of air/1 kg of fuel	10.0	20.0
2	10	P08	Lower heating value (*LHV*)	$MJ \cdot kg^{-1}$	18.0	60.0
2	11	P07	Density	$kg \cdot m^{-3}$	600.0	900.0

Table 3

Experimental parameters of diesel engine used for ANN as the output parameters

Cluster	Index	Abbr.	Parameter	Units	Interval	
					Y_{MIN}	Y_{MAX}
1	8	R04	SNO_x	$g \cdot kWh^{-1}$	0.1	20.0
2	3	R00	Smoke	m^{-1}	0.001	100.0
2	5	R02	Brake thermal efficiency (*BTE*)	-	0.01	0.5
3	2	R06	SCO_2	$g \cdot kWh^{-1}$	100.0	2000.0

3.3. Simulation routine

Table 4 delineates the methodologies used to train and validate the ANNs. During the validation phase, distinct files—0.csv (172 events), 50.csv (174 events), and 100.csv (195 events) – were used in the prediction mode while applying the same training model 200-050100.csv. Tables 6–9 represent distributions of R06, R04, R00, and R02 parameters on experiment RolNo for different types of fuel mixtures (D100, HVO50, HVO100). The selected parameters belong to two groups:

a) parameters of burning chemistry: R06 as SCO_2, R04 as *SNOx*, both in [g·kWh^{-1}], R00 as smoke, in [m^{-1}];
b) energetic parameter R02, *BTE*.

ANN consists of an input layer, a single hidden layer where the number of perceptrons M = 200 (blue), and an output layer (see Fig. 3). *VALLUM01* simulates the learning process by adjusting the weights of the artificial synapses via backpropagation. Table 4 depicts the procedure of training and validating ANNs.

The nomenclature of files was constructed according to the type of fuel mixture. 0.csv is related to the D100, 50.csv is related to the HVO50 (containing 50% HVO supplement), and 100.csv is related to the HVO100 (pure HVO). The training data file was constructed by amalgamating the contents of 0.csv, 50.csv, and 100.csv into a new file titled 050100.csv, including all entries without any selection criteria. The cumulative sum of events in the training file 050100.csv was 541 (172+174+195). The training procedure was conducted over 160,000,010 epochs using an artificial neural network with a solitary hidden layer including 200 perceptrons, exclusive to training project T0. A training stamp in the form of file 200-050100.csv (***M***=200, contains 0.csv, 50.csv, 100.csv) was obtained for validation purposes. Figure 4 depicts the variation of TNE^2 in relation to the number of epochs, demonstrating the advancement of the ANN training process.

Table 4

The training and validation of the ANNs include an input layer with 12 units, an output layer with 10 units, a hidden layer with *M* perceptrons, and a learning rate of 0.01

Project	One Hidden Layer	Training					Validation	
Name	*M*	Routine	File	Events	Epochs	TNE^2	File	Events
T0	200	T0	200-050100.cs	541	160,000,010	Fig. 4		
T0	200		200-050100.cs				0.csv	172
T50	200		200-050100.cs				50.csv	174
T100	200		200-050100.cs				100.csv	195

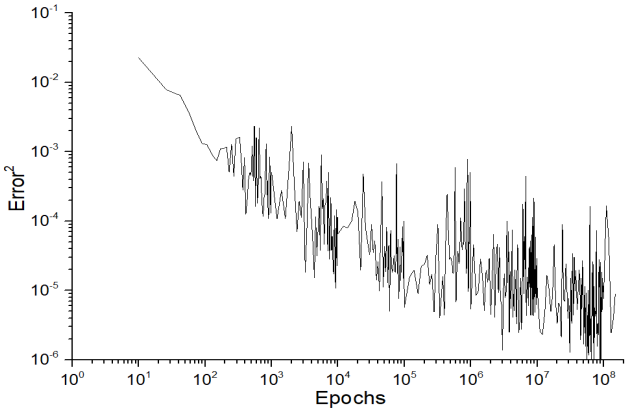

Fig. 4. TNE^2 dependence on epochs number. Evolution of the ANN training. Number of epochs: 160,000,010. Number of training events: 541. Number of perceptrons in the single hidden layer: ***M***=200

4. RESULTS

Table 5 depicts a comparative examination of the specific CO_2 emission (SCO_2) of diesel engines using three distinct fuel mixtures: D100, HVO50, and HVO100. The data are divided into two main components for each kind of fuel: the distribution of actual values and the distribution of anticipated values generated by an ANN model. Every row represents a distinct fuel combination. The scatter plots on the left-hand side of each row show the trend or distribution of SCO_2 emissions over different experimental runs (referred to as "RoINo"), with red dotted lines representing the trend or distribution. These scatter plots display peaks and troughs, which suggest fluctuations in emission rates caused by variations in operating circumstances or engine performance measures at various test points. The D100 exhibits changing amounts of SCO_2 emissions with many distinct peaks, indicating a significant degree of variability in emissions during the test cycles. The user's text is "HVO50". Like D100, the $_{SCO2}$ emissions exhibit considerable fluctuation, but the general magnitude of the peaks is considerably mitigated, indicating a potential decrease in emission levels attributable to the presence of HVO. The user has entered the text "HVO100." The fluctuation is present. However, the peaks are much reduced in comparison to D100 and HVO50, suggesting that pure HVO has the potential to generate less emissions.

The scatter plots on the right side of each row show the projected values of SCO_2 emissions compared to the actual values for each kind of fuel. These charts are essential for assessing the accuracy of the ANN predictions in comparison to the actual measured values. Each fuel type exhibits a set of graphs where data points are closely grouped around a line, indicating a significant connection between the anticipated and experimental values. This suggests that the ANN model effectively estimates $_{SCO2}$ emissions for various kinds of fuel and operating circumstances. The density of the point clusters along the 45-degree line (representing the optimal prediction line) differs somewhat across the different fuel types. The D100 points exhibit a strong alignment with the line, suggesting a high level of prediction accuracy. The HVO50 and HVO100 exhibit a strong correlation, while there are some modest variances indicating minor inaccuracies in prediction, especially at higher emission levels.

The graphical data indicates that the use of HVO, whether in the form of a mix or its pure form, in diesel engines may effectively decrease SCO_2 emissions, as seen in the emission patterns derived from the experiments. Moreover, the ANN model offers dependable forecasts of emissions, as seen by the robust correlation in the predictive graphs. This makes it a valuable tool for predicting emissions in various operating situations and with different fuel types. The efficacy of the model also underscores its potential usefulness in optimizing engine efficiency and ensuring adherence to environmental rules.

Table 6 presents an ongoing investigation of emissions from diesel engines using various fuel combinations. The analysis specifically focuses on a parameter labeled "R04," which represents the specific NO_x emissions (SNO_x). Similar to the previous diagram, the study is divided between distributions of actual values and distributions of forecasted values using ANNs for three fuel types: D100, HVO50, and HVO100.

D100 has a discernible pattern of emissions characterized by many prominent peaks of SNO_x emissions. This pattern may suggest certain operating conditions in which SNO_x levels are elevated. The variations are significant and exhibit elevated peak values. The user's text is "HVO50." Like D100, the pattern exhibits distinct peaks but with significantly lower intensity than pure diesel. This indicates that the addition of HVO assists in mitigating SNO_x emissions. HVO100 exhibits a substantial decrease in both the frequency and amplitude of peaks. The occurrence of peaks is greatly reduced in pure HVO compared to D100 and HVO50, suggesting a large decrease in SNO_x. The observed trends indicate that higher levels of HVO concentration in the fuel combination result in decreased SNO_x, which is consistent with the anticipated advantages of using cleaner and sustainable fuel sources.

The graphs located on the right side of each row represent specific fuel types and display scatter graphs comparing projected and experimental results for SNO_x emissions. Each figure has a linear regression line, which may represent a linear regression fit, illustrating the relationship between the expected and experimental values. The graphs indicate that the points are typically closely aligned along the line for all fuel types, indicating that the artificial neural networks (ANNs) can reliably forecast SNO_x emissions under various scenarios.

Concerning the forecast discrepancies of D100 and HVO50, the scatter plots demonstrate a strong correlation along the line, with a few outlier points that vary from the expected trend, particularly at higher emission levels. The user's text is "HVO100." The forecast seems to be somewhat more dispersed in comparison to D100 and HVO50, perhaps indicating difficulties in estimating emissions for a fuel variant that deviates greatly from standard diesel fuels.

Table 5

Distributions of the R06 parameter (SCO_2, g·kWh^{-1}) on experiment RolNo for different types of fuel mixtures (D100, HVO50, HVO100)

Fuel	Parameter	Distributions of predicted values
D100	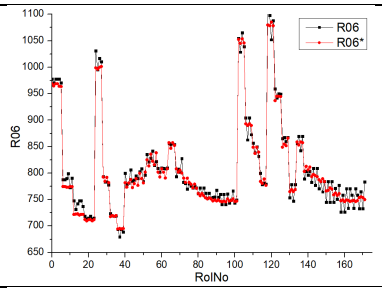	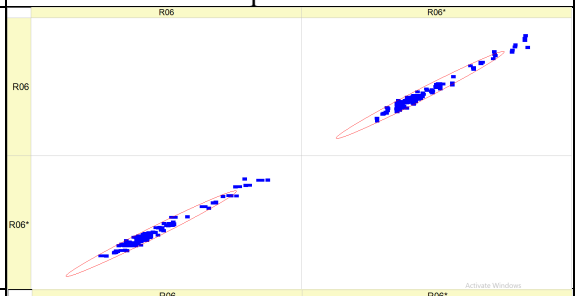
HVO50	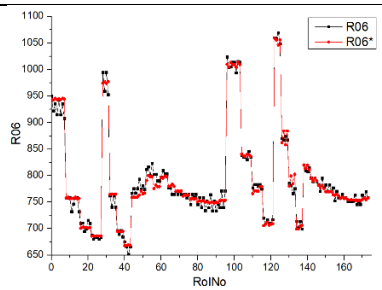	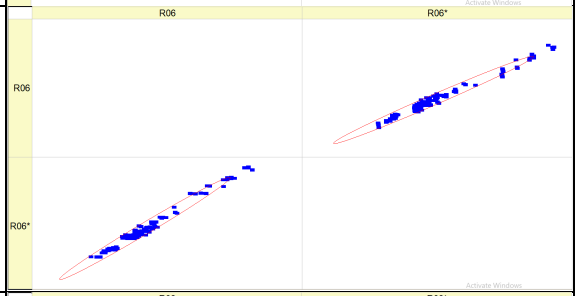
HVO100	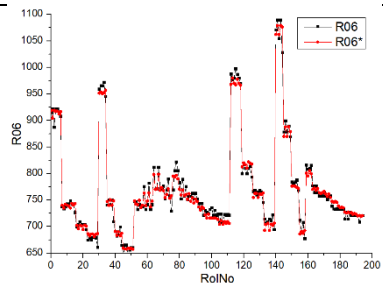	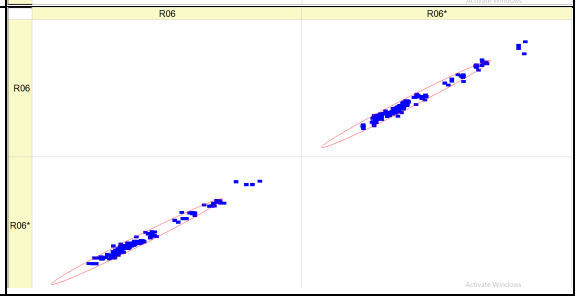

The graphical representations demonstrate that the use of HVO leads to a significant decrease in smoke emissions in diesel engines, particularly when pure HVO mixes are used. The ANN models exhibit a notable level of prediction precision, efficiently establishing the correlation between operational circumstances and emission levels. The results not only emphasize the positive impact of HVO on the environment but also demonstrate the potential of ANN models to accurately forecast engine emissions. This capability is essential for meeting regulatory requirements and optimizing engine design.

Table 7 displays statistics concerning the emissions of smoke from diesel engines while utilizing various fuel mixtures (D100, HVO50, and HVO100). The content is divided into two main parts for each kind of fuel: the distribution of actual values and the distribution of anticipated values using ANNs.

For experimental value distributions, the user's text is "D100," and the data show pronounced peaks in smoke emissions, suggesting substantial variability and instances of elevated emission levels. The distribution has many distinct peaks, which might indicate fluctuations in engine efficiency or variations in testing circumstances. The user's text is "HVO50." The figure demonstrates a significant drop in peak height when compared to D100, indicating that the presence of HVO leads to a reduction in emissions of smoke. The number of peaks is reduced, and their prominence is diminished. The HVO100 fuel has

less prominent peaks than the other two fuels, suggesting that it produces the fewest emissions related to smoke. The general trend is less pronounced, indicating that pure HVO significantly decreases the variability of emissions and the levels of peak emissions.

Table 6

Distributions of the R04 parameter (SNO_x, g·kWh^{-1}) on experiment RolNo for different types of fuel mixtures (D100, HVO50, HVO100)

Fuel	Parameter	Distributions of predicted values
D100	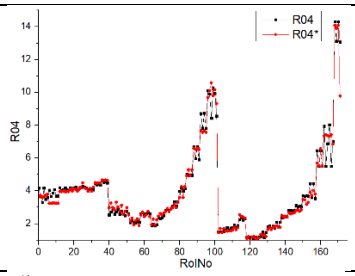	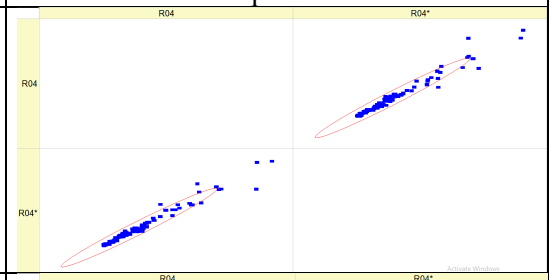
HVO50	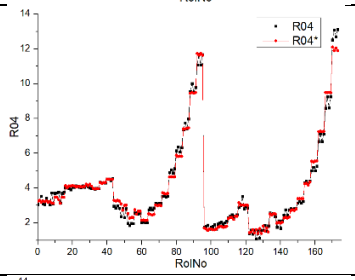	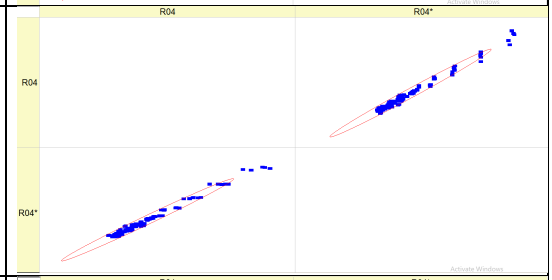
HVO100	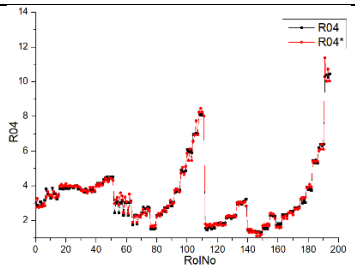	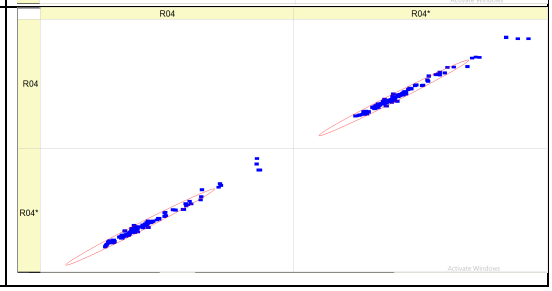

Graphs for forecasting the precision of artificial neural network models are located on the right side of the scatter graphs and compare the projected and experimental results for smoke emissions for each fuel type. The correlation analysis for each plot incorporates an oval shape that indicates the distribution and relationship of the data points to show the precision and consistency of the artificial neural networks' predictions. The D100 model has a robust linear correlation in its predictions, as seen by the dense clustering of data points along the trend line. However, slight dispersion may be noticed at higher emission levels. HVO50 has a strong prediction accuracy, as the majority of data points closely adhere to the trend line. The spread is somewhat wide, suggesting a slightly greater range of variability in forecast accuracy. For HVO100, the predictions reported here exhibit the highest degree of variation across the three fuel types, suggesting that the model's predictive accuracy may be significantly worse for pure HVO. This might be attributed to the narrower range of emission levels or distinct behavioral patterns that are less prevalent in the training data.

The investigation demonstrates a correlation between higher levels of HVO in diesel fuel and a substantial decrease in smoke emissions from engines. The decrease is seen in both the empirical data and the artificial neural network forecasts. The ANN models exhibit strong performance in forecasting smoke emissions, particularly with conventional diesel and HVO mixtures. However, they show somewhat higher variability when applied to pure HVO, indicating the need for further model tuning or more representative training data. This information is vital for promoting the use of HVO as a greener

alternative to conventional diesel backed by strong predictive models that guarantee compliance and enhance engine efficiency.

The distribution of brake thermal efficiency (*BTE*) for diesel engines running with various fuel combinations, namely D100, HVO50, and HVO100, is shown in Table 8. Additionally, the table includes the predictions produced using ANNs for these parameters.

For comparisons among different fuel types, the user's text is "D100." The figure illustrates that the *BTE* ranges mostly from roughly 0.26 to 0.34. The distribution has many peaks, indicating the variability in efficiency across various operating points or engine settings. The user's text is "HVO50." Like D100, *BTE* has a broad range but demonstrates significantly more consistency across several test points, showing less abrupt declines compared to pure diesel. The user's text is "HVO100." The efficiency distribution closely resembles that seen with HVO50, with the majority of peaks occurring at comparable values. Nevertheless, it seems to have a little more consistent efficiency profile over its working range, suggesting superior performance stability.

These patterns suggest that including HVO, whether as a mixture or in its pure form, tends to stabilize and perhaps improve the efficiency of the engine under different operating situations. Graphs forecasting the precision of ANN models are located on the right side of the scatter plots and show the projected *BTE* values versus the experimentally measured values for each fuel type. The linear trend lines in each plot demonstrate the predictive pattern and signify the level of agreement between the anticipated and actual values. There is a clear direct relationship between the projected and actual values for each kind of fuel. The points exhibit a high degree of clustering along the line, which suggests that the ANNs have a high level of predicting accuracy. The D100, HVO50, and HVO100 samples have a comparable degree of correlation, indicating that the ANNs perform the same across various fuel composition conditions. The data points consistently form compact clusters along the linear trend lines, which suggests that the forecasts are accurate.

The statistics indicate that including HVO in diesel fuel either preserves or improves the thermal efficiency of engines. Furthermore, the ANN models used for forecasting *BTE* demonstrate effectiveness across various levels of HVO concentrations, exhibiting a high degree of accuracy in their forecasts. The dependability of predictive modeling is essential for optimizing engine performance and obtaining efficiency benefits in practical applications. The results emphasize the potential advantages of using higher HVO mixes, not just for environmental benefits, but also for improved engine performance.

Table 7

Distributions of the R00 parameter (*smoke, m^{-1}*) on experiment RolNo for different types of fuel mixtures (D100, HVO50, HVO100)

Fuel	Parameter	Distributions of predicted values
D100	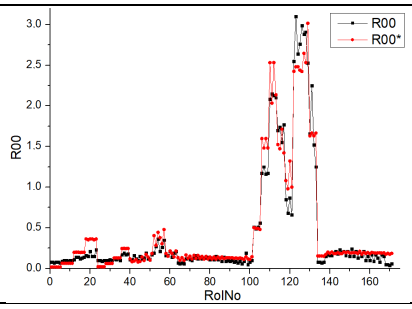	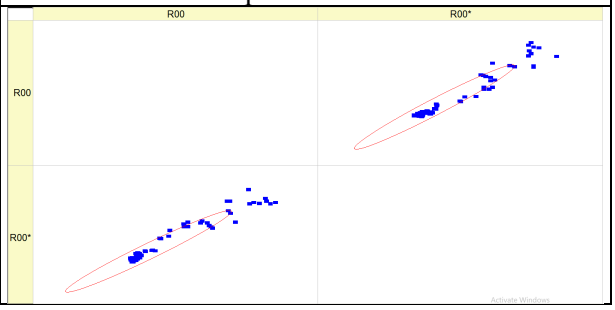

HVO50	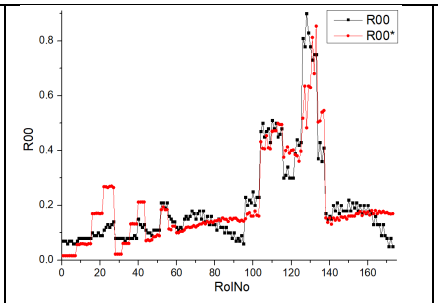	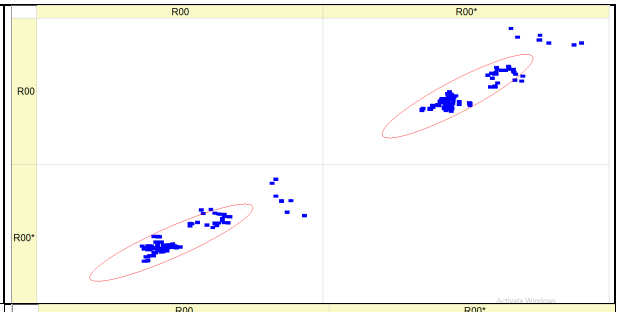
HVO100	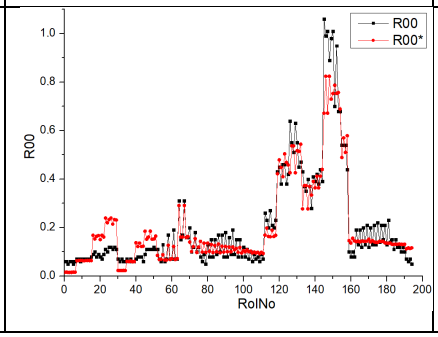	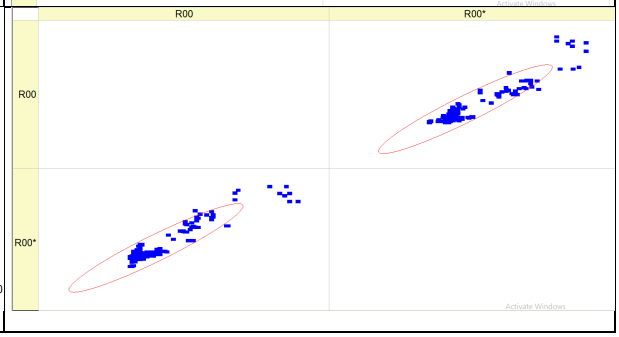

Table 8

Distributions of R02 parameter (*BTE)* on experiment RolNo for different types of fuel mixtures (D100, HVO50, HVO100)

Fuel	Parameter	Distributions of predicted values
D100	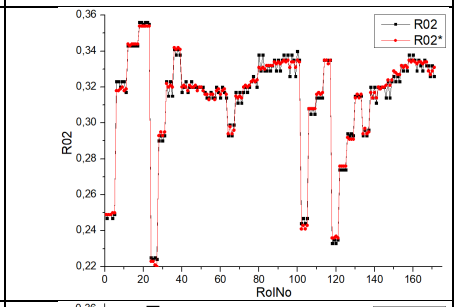	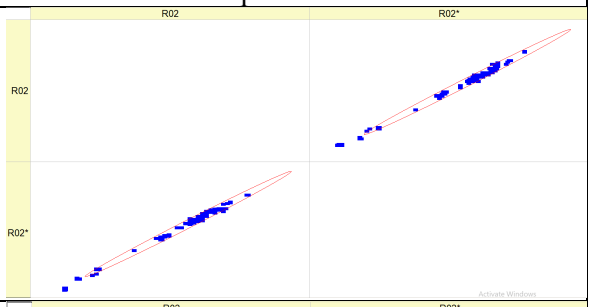
HVO50	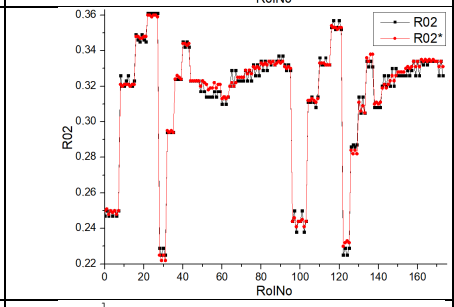	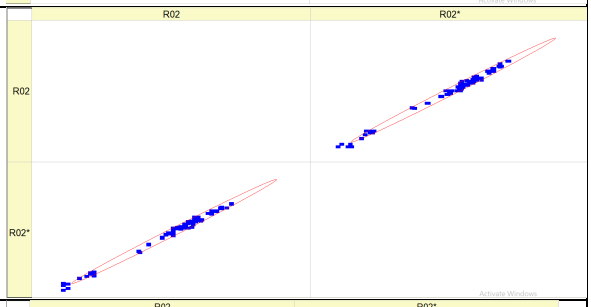
HVO100	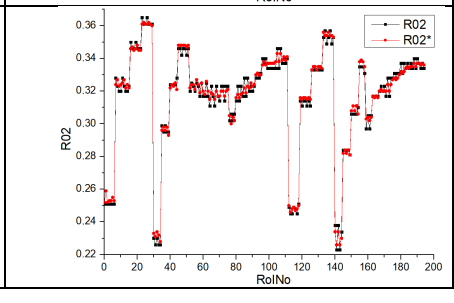	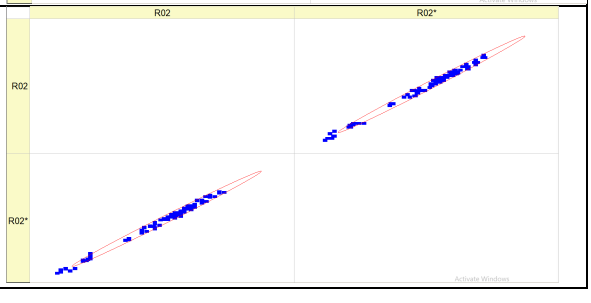

5. CONCLUSIONS

1. The quality of ANN prognosis is very high for several types of pollutants (SCO_2, SNO_x, and smoke) in diesel outcomes when diesel engine works in a wide range of regimes using different commercial fuels: D100 (pure diesel), HVO50 (containing 50% HVO supplement), HVO100 (pure HVO).
2. The relationship for chemical parameters (SCO_2, SNO_x, and smoke) related to diesel working regime and fuel type (D100, HVO50, HVO100) is satisfactory.
3. The relationship for the energetic parameter (*BTE*) related to the diesel working regime and fuel type (D100, HVO50, HVO100) is excellent.
4. For some data (input layer, number of units L = 12, output layer, number of units N = 4, number of events for training – 541), the empirically selected parameters of the ANN architecture and training regime are sufficient: single-hidden layer, number of perceptrons M = 200, training regime using 160,000,010 epochs.
5. A prognosis of outcome parameters for fuels containing HVO is available, precision is high, and deviations are less than 10%.

References

1. Aatola, H. & Larmi, M. & Sarjovaara, T. & Mikkonen, S. Hydrotreated Vegetable Oil (HVO) as a renewable diesel fuel: trade-off between NOx, particulate emission, and fuel consumption of a heavy duty engine. *SAE Int J Engines*. 2008. Vol. 1(1). P. 1251-1262. DOI: 10.4271/2008-01-2500.
2. Sunde, K. & Brekke, A. & Solberg, B. Environmental impacts and costs of hydrotreated vegetable oils, transesterified lipids and woody BTL – A Review. *Energies*. 2011. Vol. 4(6). P. 845-877. DOI: 10.3390/en4060845.
3. Bortel, I. & Vávra, J. & Takáts, M. Effect of HVO fuel mixtures on emissions and performance of a passenger car size diesel engine. *Renew Energy*. 2019. Vol. 140. P. 680-691. DOI: 10.1016/j.renene.2019.03.067.
4. Dimitriadis, A. & Natsios, I. & Dimaratos, A. & Katsaounis, D. & Samaras, Z. & Bezergianni, S. & et al. Evaluation of a hydrotreated vegetable oil (HVO) and effects on emissions of a passenger car diesel engine. *Front Mech Eng*. 2018. Vol. 4. No. 7. DOI: 10.3389/fmech.2018.00007.
5. Suarez-Bertoa, R. & Kousoulidou, M. & Clairotte, M. & Giechaskiel, B. & Nuottimäki, J. & Sarjovaara, T. & et al. Impact of HVO blends on modern diesel passenger cars emissions during real world operation. *Fuel.* 2019. Vol. 235. P. 1427-1435. DOI: 10.1016/j.fuel.2018.08.031.
6. Omari, A. & Pischinger, S. & Bhardwaj, O.P. & Holderbaum, B. & Nuottimäki, J. & Honkanen, M. Improving engine efficiency and emission reduction potential of HVO by fuel-specific engine calibration in modern passenger car diesel applications. *SAE International Journal of Fuels and Lubricants.* 2017. Vol. 10(3). No. 2017-01-2295.
7. Aakko-Saksa, P. & Murtonen, T. & Kuronen, M. & Mikkonen, S. Emissions with heavy-duty diesel engines and vehicles using FAME, HVO and GTL fuels with and without DOC+POC aftertreatment. *SAE International Journal of Fuels and Lubricants.* 2010. Vol. 2(2). P. 147-166. DOI: 10.4271/2009-01-2693.
8. Dimitriadis, A. & Seljak, T. & Vihar, R. & Žvar Baškovič, U. & Dimaratos, A. & Bezergianni, S. & et al. Improving PM-NOx trade-off with paraffinic fuels: A study towards diesel engine optimization with HVO. *Fuel*. 2020. Vol. 265. No. 116921.
9. McCaffery, C. & Zhu, H. & Sabbir Ahmed, C.M. & Canchola, A. & Chen, J.Y. & Li, C. & et al. Effects of hydrogenated vegetable oil (HVO) and HVO/biodiesel blends on the physicochemical and toxicological properties of emissions from an off-road heavy-duty diesel engine. *Fuel*. 2022. Vol. 323. No. 124283. DOI: 10.1016/j.fuel.2022.124283
10. Zoldy, M. & Szalmane Csete, M. & Kolozsi, P.P. & Bordas, P. & Torok, A. Cognitive Sustainability. *Cognitive Sustainability*. 2022. Vol. 1(1). DOI: 10.55343/cogsust.7.
11. Kozak, M. & Lijewski, P. & Fuc, P. Exhaust emissions from a city bus fuelled by oxygenated diesel. *Fuel*. 2020. No. 2020-01-2095. Available at: https://www.sae.org/content/2020-01-2095/.

12. Bereczky, A. Effect of the use of waste vegetable oil based biodiesel on the landscape in diesel engines. *Therm Sci*. 2017. Vol. 21(1 Part B). P. 567-579.
13. Žvirblis, T. & Vainorius, D. & Matijošius, J. & Kilikevičienė, K. & Rimkus, A. & Bereczky, Á. & et al. Engine vibration data increases prognosis accuracy on emission loads: a novel statistical regressions algorithm approach for vibration analysis in time domain. *Symmetry*. 2021. Vol. 13(7). No. 1234. DOI: 10.3390/sym13071234.
14. Žvirblis, T. & Hunicz, J. & Matijošius, J. & Rimkus, A. & Kilikevičius, A. & Gęca, M. Improving diesel engine reliability using an optimal prognostic model to predict diesel engine emissions and performance using pure diesel and hydrogenated vegetable oil. *Eksploat Niezawodn – Maint Reliab*. 2023. Vol. 25(4). No. 174358. DOI: 10.17531/ein/174358.
15. Mlynski, R. & Kozlowski, E. Selection of level-dependent hearing protectors for use in an indoor shooting range. *Int J Environ Res Public Health*. 2019. Vol. 16(13). No. 2266. DOI: 10.3390/ijerph16132266.
16. Kozłowski, E. & Borucka, A. & Świderski, A. Application of the logistic regression for determining transition probability matrix of operating states in the transport systems. *Eksploat Niezawodn – Maint Reliab*. 2020. Vol. 22(2). P. 192-200. DOI: 10.17531/ein.2020.2.2.
17. Borucka, A. & Kozłowski, E. & Parczewski, R. & Antosz, K. & Gil, L. & Pieniak, D. Supply sequence modelling using Hidden Markov Models. *Appl Sci*. 2022. Vol. 13(1). No. 231. DOI: 10.3390/app13010231.
18. Yang, R. & Yan, Y. & Sun, X. & Wang, Q. & Zhang, Y. & Fu, J. & et al. An artificial neural network model to predict efficiency and emissions of a gasoline engine. *Processes*. 2022. Vol. 10(2). No. 204. DOI: 10.3390/pr10020204.
19. Buscema, M. Back Propagation Neural Networks. *Subst Use Misuse*. 1998. Vol. 33(2). P. 233-270.
20. Sekhar Ch. & Meghana P.S. A study on backpropagation in artificial neural networks. *Asia-Pac J Neural Netw Its Appl.* 2020. Vol. 4(1). P. 21-28.
21. Murat, H.S. A brief review of feed-forward neural networks. *Commun Fac Sci Univ Ank.* 2006. Vol. 50(1). P. 11-17.
22. Zhang, Z. & Feng, F. & Huang, T. FNNS: An effective feedforward neural network scheme with random weights for processing large-scale datasets. *Appl Sci*. 2022. Vol. 12(23). No. 12478. DOI: 10.3390/app122312478.
23. Karunamurthy, K. & Janvekar, A.A. & Palaniappan, P.L. & Adhitya, V. & Lokeswar, T.T.K. & Harish, J. Prediction of IC engine performance and emission parameters using machine learning: A review. *J Therm Anal Calorim*. 2023. Vol. 148(9). P. 3155-3177.
24. Gruodis, A. Realizations of the artificial neural network for process modeling. overview of current implementations. *Appl Bus Issues Solut.* 2023. Vol. 2. P. 22-27. DOI: 10.57005/ab.2023.2.3.
25. Gruodis, Alytis. VALLUM01. *Advanced tool for implementation of Artificial Neural Network containing tabular interface for input/output*. Vilnius, Lithuania; 2023.
26. Gruodis, A. *Advanced Tool for Implementation of Artificial Neural Network Containing Tabular Interface for Input/Output 2023*. Vilnius, Lithuania. 2024. Available at: https://github.com/solo51/VALLUM.
27. Matijošius, J. & Rimkus, A. & Gruodis, A. Validation challenges in data for different diesel engine performance regimes utilising HVO fuel: a study on the application of artificial neural networks for emissions prediction. *Machines.* 2024. Vol. 12(4). No. 279. DOI: 10.3390/machines12040279.
28. Matijošius, J. & Rimkus, A. & Gruodis, A. Validation of ecology and energy parameters of diesel exhausts using different fuel mixtures, consisting of hydrogenated vegetable oil and diesel fuels, presented at real market: approaches using artificial neural network for large-scale predictions. *Machines.* 2024. Vol. 12(6). No. 353. DOI: 10.3390/machines12060353.

Received 19.06.2023; accepted in revised form 26.11.2024